SCIENTIFIC REPORTS

OPEN

Hartman effect for spin waves in exchange regime

Jarosław W. Kłos[1,2], Yuliya S. Dadoenkova[3,4], Justyna Rychły[1], Nataliya N. Dadoenkova[3,4], Igor L. Lyubchanskii[4,5] & Józef Barnaś[1,6]

Received: 22 January 2018
Accepted: 5 November 2018
Published online: 18 December 2018

Hartman effect for spin waves tunnelling through a barrier in a thin magnetic film is considered theoretically. The barrier is assumed to be created by a locally increased magnetic anisotropy field. The considerations are focused on a nanoscale system operating in the exchange-dominated regime. We derive the formula for group delay τ_{gr} of a spin wave packet and show that τ_{gr} saturates with increasing barrier width, which is a signature of the Hartman effect predicted earlier for photonic and electronic systems. In our calculations, we consider the general boundary conditions which take into account different strength of exchange coupling between the barrier and its surrounding. As a system suitable for experimental observation of the Hartman effect we propose a CoFeB layer with perpendicular magnetic anisotropy induced by a MgO overlayer.

The problem of quantum tunnelling of a particle through a potential barrier higher than the particle energy is one of the fundamental problems in quantum mechanics[1–4]. More than half a century ago Hartman considered analytically tunnelling of a Gaussian wave packet through a rectangular potential barrier of thickness L in metal/insulator/metal junctions[5]. He derived a formula for the group delay τ_{gr}, i.e. the time in which the incident packet travels from the first border of the barrier at $x=0$ to the second one at $x=L$. He concluded that the group delay τ_{gr} saturates with increasing barrier thickness, which means that for thick barriers the group delay is shorter than the time required by the packet to traverse the distance L in the corresponding uniform (no barrier) material. This phenomenon is known as the Hartman effect (HE).

However, tunnelling is a wave phenomenon which refers to various kinds of waves, including also wave functions of quantum particles. In general, the tunnelling takes place when the wave passing through the barrier has the form of exponentially evanescent function, and then continues the propagation as an ordinary wave (in oscillatory form) with reduced amplitude and shifted phase. The Hartman's paper initiated a huge activity in different fields: including (i) tunnelling of electromagnetic Gaussian wave packets in various structures like photonic crystals (see, for example, review articles[4,6–12] and research papers[7,13–16]), (ii) tunnelling of acoustical and optical phonons[17,18], and (iii) tunnelling of electrons in graphene[19–23]. For all types of the above mentioned waves, the saturation of group delay with increasing barrier width is observed in tunnelling processes. This feature leads to a counter-intuitive conclusion on *an unlimited increase of propagation speed* of tunnelling wave packets. This paradox was the subject of intensive scientific debate[24] and was explained using the arguments referring to a reshaping of the wave packets[25] or to the saturation of energy deposition within the barrier[26].

The HE was not studied yet in the case of spin waves (SWs), although the effects related to tunnelling, trapping and mastering of propagation time or velocity for SWs in non-uniform magnetic structures have been already investigated theoretically and experimentally. Most of the experimental studies were performed for dipolar SWs in structures based on yttrium- iron garnet (YIG) or on permalloy. Tunnelling of SW was investigated experimentally in YIG stripes with a single[27] (or double[28]) barrier formed by the Oersted field or in YIG film with a mechanical gap[29]. There are also reports which show that the group delay or group velocity for SWs in periodic structures can be significantly changed in comparison to those in homogeneous systems[30–33].

In this paper we consider HE for SWs tunnelling through a barrier in a thin magnetic film with perpendicular magnetic anisotropy (PMA). We restrict our considerations to an exchange-dominated region of the spin wave spectrum. We demonstrate theoretically the saturation of the group delay for exchange SWs with increasing width

[1]Faculty of Physics, Adam Mickiewicz University in Poznań, 61-614, Poznań, Poland. [2]Institute of Physics, University of Greifswald, 17489, Greifswald, Germany. [3]Ulyanovsk State University, 432017, Ulyanovsk, Russia. [4]Donetsk Institute for Physics and Engineering named after O.O. Galkin, NAS of Ukraine, 03680 Kiev, Ukraine. [5]Faculty of Physics, V. N. Karazin Kharkiv National University, 61022, Kharkiv, Ukraine. [6]Institute of Molecular Physics, Polish Academy of Sciences, 60-179, Poznań, Poland. Correspondence and requests for materials should be addressed to J.W.K. (email: klos@amu.edu.pl)

of the barrier, which is an evident signature of HE. The *barrier* can be created by a local increase of the internal field, which can be caused by a change (increase) of the magnetocrystalline anisotropy within the barrier. Such a barrier can be formed, for instance, using a material with anisotropy higher than that in the remaining (left and right) parts of the junction (referred to in the following as *matrix*). However, to reduce spin wave scattering at the barrier/matrix interfaces, one can take a uniformly magnetized thin film of a material with low damping, and then, with etching techniques, fabricate a narrow stripe of reduced thickness. By covering the film with an insulating material, one can induce an interface anisotropy, which in a narrow stripe can be different (enhanced) from that in the other parts of the structure. Indeed, for a layer (up to a few nanometers thick) the main contribution to the effective magnetic anisotropy originates from surfaces and/or interfaces, which grows with decreasing layer thickness. More details on the system proposed for experimental investigations of HE are given in the next section.

For dipolar spin waves we can form the barrier in a few other ways. If we consider the magnetic stripe of high magnetization saturation surrounded by two magnetic half-planes made of material of lower magnetization saturation then, in the range between FMR frequencies of this two materials, the spin wave tunnelling can be observed – the Demon-Eshbach modes will be evanescent in the barrier (stripe) and oscillating in the matrix (surrounding material). We suspect that for such system the Hartman effect should be also observed. The other the magnonic systems in which the Hartman effect is expected to be found are the structures with air gaps where the exponentially decaying magnetostatic potential (and associated dynamic demagnetizing field) can couple the spin wave dynamics across the air gap. The magnonic systems operating in the dipolar regime are, in most cases, much easier for fabrication than the extremely small systems working in exchange regime. However, the theoretical description dipolar system is more challenging. Therefore we decided to start, in this paper, from the theoretical and numerical studies of Hartman effect for exchange waves.

The paper is organized as follows. The system under consideration is described in the section "The Model". In the next section, we present a theoretical description. In this section we discuss the propagation of exchange SWs in the case of spatially dependent anisotropy field. We also outline the theoretical basis of the HE for SWs. Numerical results and their discussion are presented in the subsequent section. The last section contains the summary and final conclusions. The manuscript is supplemented by the discussion of boundary conditions for SWs in exchange regime and technical details concerning the derivation of the transmissivity function.

The Model

The system under consideration, presented schematically in Fig. 1a, is planar. Both external magnetic field $\boldsymbol{H}_0$ and effective anisotropy field $\boldsymbol{H}_a(x)$ are oriented out-of-plane. We assume a one-dimensional magnetic barrier in the form of a stripe region, in which (for $0 < x < L$) the effective anisotropy field $H_a(x)$ is increased. The barrier is rectangular, i.e. H_a changes abruptly at $x = 0$ and $x = L$, see Fig. 1b. We also assume that the magnetization M_S and exchange length λ_{ex} in the barrier region are changed (reduced) in reference to the matrix regions ($x < 0$ and $x > L$), see Fig. 1c.

Thickness of the magnetic layer is much smaller than the considered wavelength of SWs and also smaller than the width of the barrier L. This allows to neglect the spatial changes of spin wave amplitude across the magnetic layer (regardless of the partial pinning which exists due to the interfacial anisotropy K_i between the magnetic layer and nonmagnetic overlayer). To simplify our analysis, we investigate SWs propagating perpendicularly to the barrier only, which effectively reduces the problem to the one-dimensional one.

To take into account the in-plane inhomogeneity of the magnetic material, which in real systems can be observed at the interfaces between the matrix and barrier, we introduce the exchange coupling at these interfaces as an additional parameter of our model. The strength of this exchange coupling is important for determining the interfacial boundary conditions for SWs. These boundary conditions significantly influence the phase factor of the transmissivity $T(\omega)$[34–37], which, in turn, is crucial for the determination of the group delay $\tau_{gr}(\omega)$ of SWs tunnelling (propagating) through (over) the barrier[24]. Therefore, one can expect that the HE (i.e. saturation of τ_{gr} with increasing width of the barrier L) is sensitive to a particular formulation of the boundary conditions for SWs.

For a prospective experimental realization of the considered system we need a material characterized by a high out-of-plane anisotropy field, which additionally ensures low SW damping. A suitable system with PMA is a thin CoFeB layer covered with MgO. The effect of PMA induced at the CoFeB/MgO interface is well known and was already used in spintronics for fabrication of magnetic tunnel junctions of reduced dimensions[38]. The interfacial anisotropy K_i depends critically on the crystalline structure and bonding at the CoFeB/MgO interfaces. It grows initially with increasing thickness of the MgO layer and then decreases for larger thicknesses, when crystalline MgO starts to form[39]. For positive values of the energy density (effective anisotropy) $K = K_i/t_{CoFeB} - \mu_0 M_S^2/2$, the magnetic easy-axis is oriented out-of-plane and the system is magnetized perpendicularly in the absence of an external field. Thus, by appropriate tuning of the MgO thickness and of the CoFeB thickness (t_{CoFeB}), one can increase the effective anisotropy inside the stripe region and form the barrier (see Fig. 1).

In the following sections we will consider the propagation of exchange SWs in a nonuniform profile of effective (out-of-plane) anisotropy field $H_a = 2K_i/(\mu_0 M_S t_{CoFeB}) - M_S$, additionally shifted by a spatially homogeneous external field H_0 (applied in the same direction). We will show that the field $H = H_a(\boldsymbol{r}) + H_0$ can be treated as a counterpart of electrostatic potential $V(\boldsymbol{r})$ for electronic waves. In the *magnetic barrier*, where the spin wave frequency ω fulfils the condition $\gamma\mu_0\omega < H_0 + H_a(\boldsymbol{r})$, the spin wave profile has evanescent character, typical for tunnelling of electronic waves of energy $E < V(\boldsymbol{r})$. We will exploit this formal similarity of electronic waves and exchange SWs to discuss HE for magnonics.

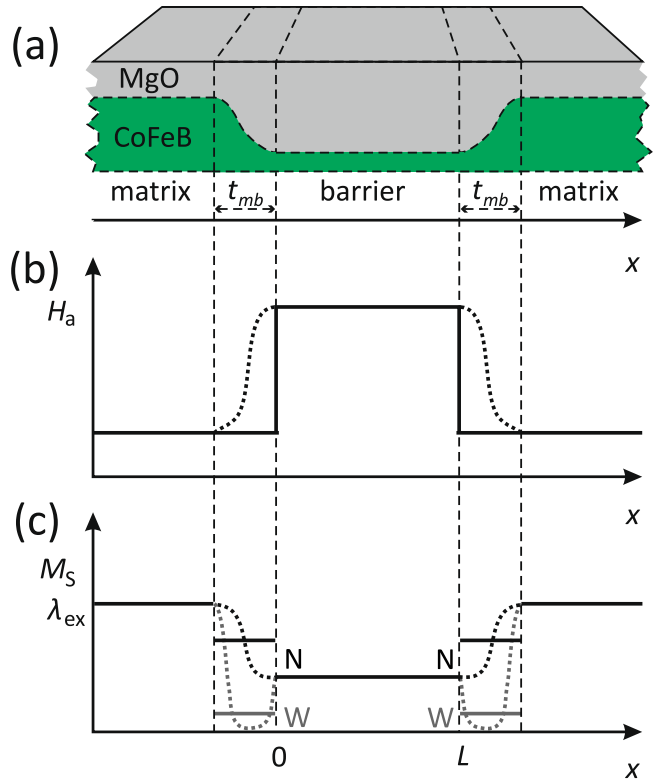

Figure 1. Schematic of the system under consideration. (**a**) The exemplary structure has the form of a ferromagnetic layer made of a low-damping material (CoFeB) with an out-of-plane magnetic anisotropy induced by the interface with the oxide layer (MgO) deposited on top of the ferromagnetic layer. The groove in the ferromagnetic layer makes the effective anisotropy field H_a higher, forming the barrier (**b**) due to a larger contribution of the CoFeB/MgO interface anisotropy to H_a. The change in thickness of the magnetic layer can also modify other material parameters (**c**): saturation magnetisation M_S and exchange length λ_{ex}. In the calculations we used a simplified model with abruptly changing material parameters (solid lines). We also assumed that the material parameters at the interfaces between the barrier and matrix ($M_{S,mb}$, $\lambda_{ex,mb}$) can be different from the bulk parameters, and can correspond to the weak (W) or natural (N) exchange coupling between the barrier and the matrix.

Theoretical description

In order to discuss HE for exchange dominated the SWs, we start from the derivation of an analytic formula for the transmissivity function $T(\omega)$ through a magnetic barrier embedded in a magnetic matrix, taking into account different types of boundary conditions at the barrier/matrix interfaces. Then, we derive the formula for the group delay τ_{gr} for spin wave packet tunnelling (propagating) through (over) the magnetic barrier. Finally, we discuss the HE for exchange dominated SWs by analyzing the formula for group delay in the limit of wide barriers.

Exchange spin waves in spatially dependent anisotropy field. In general, the magnetization dynamics in a magnonic system is described by the Landau-Lifshitz equation, which has the following form in the absence of damping:

$$\frac{\partial \boldsymbol{M}(\boldsymbol{r}, t)}{\partial t} = -\gamma\mu_0 \boldsymbol{M}(\boldsymbol{r}, t) \times \boldsymbol{H}_{\text{eff}}(\boldsymbol{r}, t), \tag{1}$$

where $\boldsymbol{M}$ and $\boldsymbol{H}_{\text{eff}}$ stand for the magnetization and the effective magnetic field, respectively, and γ is the gyromagnetic ratio. We consider a system in which the SWs of short wavelengths propagate in a magnetic layer with spatially varying (along with the x-direction) material parameters: saturation magnetization $M_S(x)$, magnetic anisotropy $H_a(x)$, and exchange length $\lambda_{ex}(x)$. We assume that the effective field, $\boldsymbol{H}_{\text{eff}} = \boldsymbol{H}_0 + \boldsymbol{H}_a + \boldsymbol{H}_{ex}$, includes the contributions from a uniform static external magnetic field $\boldsymbol{H}_0 = [0, 0, H_0]$, static and spatially dependent effective anisotropy field $\boldsymbol{H}_a(x) = [0, 0, H_a(x)]$, and the dynamical term due to the exchange interaction between magnetic moments, $\boldsymbol{H}_{ex}(x, t)$. The latter term can be written as[40]:

$$\boldsymbol{H}_{ex}(x, t) = \nabla\lambda_{ex}^2(x)\nabla\boldsymbol{M}(x, t), \tag{2}$$

where the magnetization $\boldsymbol{M}(x, t)$ precesses around the effective field $\boldsymbol{H}_{\text{eff}}$, $\boldsymbol{M}(x, t) \approx [m_x(x)e^{i\omega t}, m_y(x)e^{i\omega t}, M_S]$.

When considering the propagation of SWs in the x-direction (normal to the barrier), the linearized Landau-Lifshits equation can be written in the form:

$$i\frac{\omega}{\gamma\mu_0}m_x(x) = M_S(x)\frac{\partial}{\partial x}\lambda_{ex}^2(x)\frac{\partial}{\partial x}m_y(x) - m_y(x)\left(\frac{\partial}{\partial x}\lambda_{ex}^2(x)\frac{\partial}{\partial x}M_S(x) + H_0 + H_a(x)\right),$$
$$i\frac{\omega}{\gamma\mu_0}m_y(x) = -M_S(x)\frac{\partial}{\partial x}\lambda_{ex}^2(x)\frac{\partial}{\partial x}m_x(x) + m_x(x)\left(\frac{\partial}{\partial x}\lambda_{ex}^2(x)\frac{\partial}{\partial x}M_S(x) + H_0 + H_a(x)\right). \quad (3)$$

Substituting: $m_+(x) = m_x(x) + im_y(x)$ and $m_-(x) = m_x(x) - im_y(x)$ we can write Eq. (3) in the following, more compact form:

$$-\frac{d}{dx}\lambda_{ex}^2(x)\frac{d}{dx}m_\pm(x) + v(x)m_\pm(x) = M_S^{-1}(x)\left(\pm\frac{\omega}{\gamma\mu_0}\right)m_\pm(x), \quad (4)$$

where:

$$v(x) = M_S^{-1}(x)\left(H_0 + H_a(x) + \frac{d}{dx}\lambda_{ex}^2(x)\frac{d}{dx}M_S(x)\right). \quad (5)$$

Equation (4) has the mathematical form of Sturm-Liouville equation, and therefore it possesses the properties of other differential equations of a similar kind (e.g. of the Schrödinger equation). One can identify $\lambda_{ex}^2(x)$ and $v(x)$ as counterparts of the inverse effective mass and the effective potential, respectively. The last term in Eq. (5) contributes to the *effective potential* $v(x)$ only at the interfaces, at which the material parameters (λ_{ex}^2, M_S) change. The formal similarity of Eq. (4) to Schrödinger equation allows one to expect the HE for exchange SWs tunnelling through a barrier, as well.

To find the solution of Eq. (4) in the whole system (see Fig. 1), one has to match the solutions in homogeneous materials of the barrier and of the surrounding medium (matrix). For the barrier and matrix one can write Eq. (4) for m_+ as:

$$-\widetilde{M}_{S,\alpha}\lambda_{ex,\alpha}^2\frac{d^2}{dx^2}m_+(x) + (1 + \widetilde{H}_{a,\alpha})m_+(x) = \Omega m_+(x), \quad (6)$$

where $\alpha = \{m, b\}$ refers to the matrix (m) or barrier (b), respectively. The exchange lengths $\lambda_{ex,m}$ in the matrix and $\lambda_{ex,b}$ in the barrier are measured in the units of spatial coordinate x. In turn, $\widetilde{M}_{S,\alpha}$ and $\widetilde{H}_{a,\alpha}$ denote the dimensionless saturation magnetization and effective anisotropy field, respectively, for the matrix or barrier:

$$\widetilde{M}_{S,\alpha} = \frac{M_{S,\alpha}}{H_0},\ \widetilde{H}_{a,\alpha} = \frac{H_{a,\alpha}}{H_0}, \quad (7)$$

whereas Ω is the dimensionless frequency:

$$\Omega = \frac{\omega}{\gamma\mu_0 H_0}. \quad (8)$$

The general solution of Eq. (6) takes the form:

$$m_+(x) = C_1 e^{ik_\alpha x} + C_2 e^{-ik_\alpha x}, \quad (9)$$

where C_1 and C_2 are certain integration constants, while k_α is the wave number which can be written in the form:

$$k_\alpha(\Omega) = \lambda_{ex,\alpha}^{-1}\widetilde{M}_{S,\alpha}^{-\frac{1}{2}}\sqrt{\Omega - (1 + \widetilde{H}_{a,\alpha})}. \quad (10)$$

Transmissivity and group delay. Let's consider now the incident SW $e^{i(k_m x + \Omega t)}$ of frequency $\Omega > 1 + \widetilde{H}_{a,m}$, propagating from the left side ($x < 0$) towards the barrier. Here, time t is given in the units of $(H_0\gamma\mu_0)^{-1}$. The wave reflected from the barrier can be written as $R\,e^{i(-k_m x + \Omega t)}$, where R is a complex amplitude. In the barrier region ($0 < x < L$), the corresponding solution takes the form of the wave combination given in Eq. (9), $(C_1 e^{ik_b x} + C_2 e^{-ik_b x})e^{i\Omega t}$, where the evanescent solutions (with real exponents $\pm ik_b$) appear in the tunnelling regime, i.e. for $1 + \widetilde{H}_{a,m} < \Omega < 1 + \widetilde{H}_{a,b}$. In turn, the transmitted SW $T\,e^{i(k_m x + \Omega t)}$ is observed on the opposite side of the barrier (for $x > L$) with the complex amplitude T.

The transmissivity $T(\Omega, L)$ can be obtained by matching the solutions at the interfaces between the barrier and matrix: (i) $(e^{ik_m x} + Re^{-ik_m x})e^{i\Omega t}$ with $(C_1 e^{ik_b x} + C_2 e^{-ik_b x})e^{i\Omega t}$ at $x = 0$ and (ii) $(C_1 e^{ik_b x} + C_2 e^{-ik_b x})e^{i\Omega t}$ with $Te^{i(k_m x + \Omega t)}$ at $x = L$. To match the solutions we have to apply appropriate boundary conditions. The general formulation of the boundary conditions for exchange SWs should take into account possible change of exchange coupling at interfaces between the barrier and matrix. This coupling affects the phase shift acquired by SW when it passes through the interface, and thus modifies the group delay τ_{gr}. In our calculations we used Barnas-Mills boundary conditions (BMBC)[41,42], which include the modification of exchange interaction at the interfaces both in the weak and strong coupling regime (see the Supplemantary Information for details). Using BMBC one finds the transmissivity $T(\Omega, L)$ in the form:

$$T(\Omega, L) = \frac{e^{-ik_m L}}{\Delta_c \cos(k_b L) + i\Delta_s \sin(k_b L)}, \tag{11}$$

where $\Delta_s(k_m, k_b)$ and $\Delta_c(k_m, k_b)$ are the rational expressions of the form depending on the boundary conditions on the interface between matrix and barrier (see Supplementary Information for details).

The transmissivity $T(\Omega, L)$ is one of the most important spectral characteristics of the system. Its magnitude $|T(\Omega, L)|$ gives the information about the energy density, which is transmitted through/over the barrier. For Eq. (11), we can write the following expression for $|T(\Omega, L)|$:

$$|T(\Omega, L)| = |\Delta_c \cos(k_b L) + i\Delta_s \sin(k_b L)|^{-1}. \tag{12}$$

It is worth to notice that the transmissivity $T(\Omega, L)$ depends on the barrier width L only through the factors: $\sin(k_b L)$, $\cos(k_b L)$ and $\exp(k_m L)$, presented explicitly in Eq. (11).

The group delay τ_{gr} depends on the phase of the transmissivity function. Following ref.[24], we find $\tau_{gr}(\Omega, L)$ in the form:

$$\tau_{gr}(\Omega, L) = \frac{1}{\gamma\mu_0 H_0}\frac{d}{d\Omega}[\mathrm{Arg}(T) + k_m L]. \tag{13}$$

In the following, we will use the dimensionless group delay $\tilde{\tau}_{gr}(\Omega, L)$, defined as:

$$\tilde{\tau}_{gr}(\Omega, L) = \gamma\mu_0 H_0 \tau_{gr}. \tag{14}$$

The phase $\phi = \mathrm{A}rg(T) + k_m L$, gained by SW after tunnelling (propagating) through (over) the barrier, consists of two terms. The term $k_m L$ is a *geometrical* phase, which would be acquired by the SW on the distance L (width of the barrier) in the absence of the barrier, i.e. propagating in a homogeneous medium described by the material parameters of the matrix. The other term describes the phase shift resulting from the presence of the barrier. By referring to Eq. (11) we can notice that the phase ϕ can only be expressed by the argument of the denominator, $\Delta_c\cos(k_b L) + i\Delta_s\sin(k_b L)$. This allows writing Eq. (13) in a more explicit form:

$$\tilde{\tau}_{gr}(\Omega, L) = -\frac{d}{d\Omega}[\mathrm{Arg}(\Delta_c \cos(k_b L) + i\Delta_s \sin(k_b L))]. \tag{15}$$

Hartman effect. For tunnelling SWs, the wave number k_b is purely imaginary:

$$k_b = i\kappa_b, \tag{16}$$

where κ_b is real. Therefore, for a wide barrier ($L \gg 1/\kappa_b$), one can make the following simplifications in Eq. (15): $\cos(k_b L) = \cosh(\kappa_b L) \approx \frac{1}{2}e^{\kappa_b L}, \sin(k_b L) = i\sinh(\kappa_b L) \approx \frac{1}{2}ie^{\kappa_b L}$. This brings us to the conclusion that the group delay $\tilde{\tau}_{gr}$ will saturate with increasing barrier width ($L \to \infty$), which is the essence of the *Hartman effect*. In this limit, the group delay becomes independent on the barrier width:

$$\tilde{\tau}_{gr}(\Omega) \underset{L\to\infty}{=} -\frac{d}{d\Omega}[\mathrm{Arg}(\Delta_c - \Delta_s)]. \tag{17}$$

It can be proved that the group delay in the tunnelling regime is always positive. Thus, the controversies related to the Hartman effect (including the discussion about the violation of causality) have nothing to do with negative group delay. In the limit $L \to \infty$ the group delay diverges at the ranges of tunnelling regime, for $\Omega = 1 + \widetilde{H}_{a,m}$ and $\Omega = 1 + \widetilde{H}_{a,b}$.

One of the main obstacles making the observation of the HE difficult is the low magnitude of the transmissivity $|T(\Omega, L)|$ in the tunnelling regime, which decays exponentially with increasing barrier width L for $L \gg 1/k_b$, where one finds:

$$|T(\Omega, L)| \underset{L\gg 1/\kappa_b}{=} e^{-\kappa_b L}|\Delta_c - \Delta_s)|^{-1}. \tag{18}$$

Therefore, it is useful to define the so-called figure-of-merit (FOM) for the HE:

$$\mathrm{FOM} = \frac{|T|}{\tilde{\tau}_{gr}}. \tag{19}$$

The high value of the FOM points out the parameters of the model for which the short group delay coincides with the relatively high magnitude of the transmissivity.

The HE can be also observed for reflected waves, where the group delay is defined as[24]:

$$\tau'_{gr}(\Omega, L) = \frac{1}{\gamma\mu_0 H_0}\frac{d}{d\Omega}[\mathrm{Arg}(R)]. \tag{20}$$

The complex coefficient R is the reflectivity (see the discussion the beginning of this section). For a symmetric barrier, the group delays for transmitted waves τ_{gr} and for reflected waves τ'_{gr} are equal[43,44]. This also means that

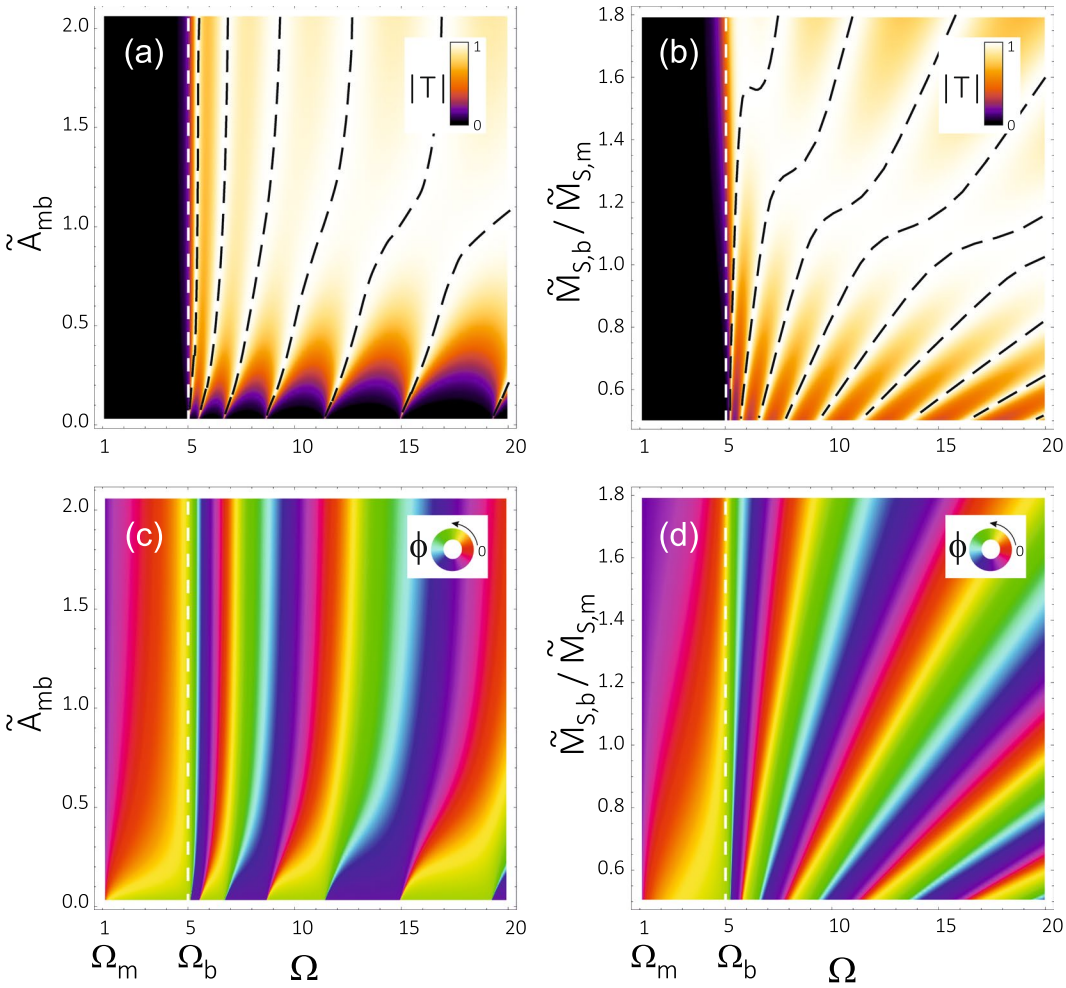

Figure 2. The absolute value of the transmissivity $|T|$ (**a**,**b**) and the phase ϕ gained in the transmission (**c**,**d**) for the anisotropy barrier of height $\widetilde{H}_{a,b}+1=5$ and width $L=5$, separated from the matrix by an interface layer of width $t=0.25$ (widths are given in the units of λ_{ex}). Both $|T|$ and ϕ are presented as a function of the spin wave frequency Ω and material parameters: the strength of the interface exchange coupling, $\widetilde{A}_{mb}=\lambda^2_{ex,mb}\widetilde{M}^2_{S,mb}$ (**a**,**c**) and the magnetization contrast between the barrier and matrix, $\widetilde{M}_{S,b}/\widetilde{M}_{S,m}$ (**b**,**d**). Black dashed lines in (**a**,**b**) mark the maxima ($|T|=1$) of the transmissivity. The frequencies $\Omega_m=\widetilde{H}_{a,m}+1=1$ and $\Omega_b=\widetilde{H}_{a,b}+1=5$ denote the minimum frequency for the propagating exchange SWs in homogeneous materials of the matrix and barrier, respectively. The later one is marked additionally by vertical white dashed line. The calculations have been done for the same values of exchange length $\lambda_{ex}=1$ in the barrier and in the matrix. The width of the barrier and the exchange length are measured in the same a.u. of length.

for the barrier characterized by a symmetric shape of the effective anisotropy field: $H_a(L/2+x)=H_a(L/2-x)$ and identical boundary conditions at $x=0$, L, the saturated values of the group delay for transmitted and reflected waves will be also equal.

Numerical Results

Now we present numerical results obtained for the system under consideration. In Fig. 2 we show the absolute value of the transmissivity $|T|$ (a, b) and the phase $\phi=Arg(T)+k_mL$ gained by SW transmitted through (or over) the magnetic barrier (b, d) – both as a function of the frequency Ω and two selected model parameters (one of interface and another one of bulk character). More specifically, we show there the impact of interface exchange coupling (defined as $\widetilde{A}_{mb}=\lambda^2_{ex,mb}M^2_{S,mb}/H_0^2$ – see Fig. 1 and Supplementary Information) (a, c), and the influence of a contrast between the bulk saturation magnetization of the barrier, $M_{S,b}$, and of the matrix, $M_{S,m}$ (c,d). The results have been obtained with the use of general BMBC. These conditions, however, comprise other types of the boundary conditions considered here (see Supplementary Information).

Transmission in the tunnelling regime (under barrier), i.e. for frequencies $\Omega<\Omega_b=\widetilde{H}_{a,b}+1)$, is very small, but it increases rapidly for Ω approaching Ω_b ($\Omega_b=5$ in Fig. 2). This increase is less rapid for stronger exchange coupling between the barrier and matrix (see Fig. 2a), and for the saturation magnetization in the barrier larger than that in the matrix region (see Fig. 2b).

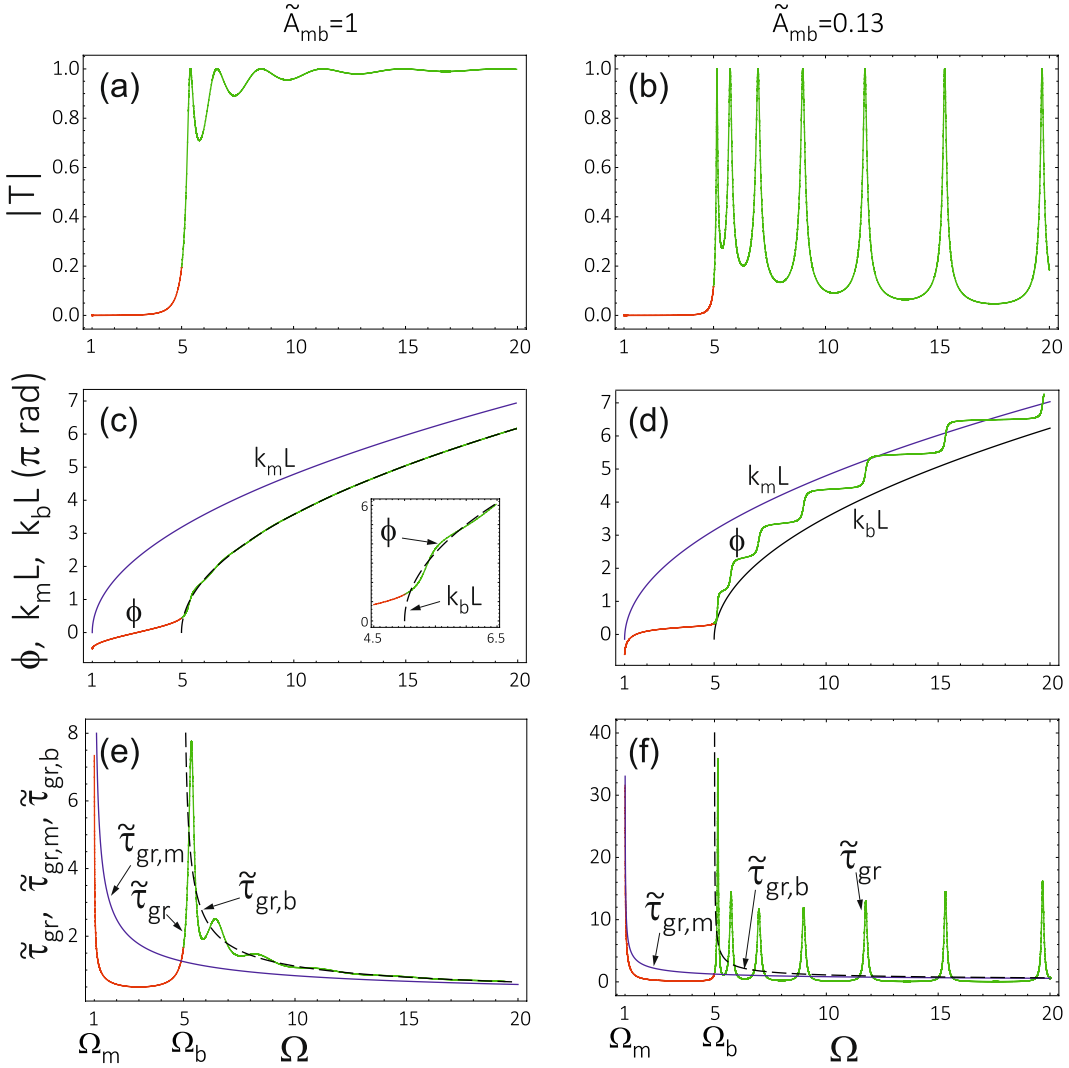

Figure 3. The absolute value of the transmissivity $|T|$ (**a**,**b**), the phase ϕ gained in the transmission (**c**,**d**), and the corresponding group delay (**e**,**f**) shown as a function of the spin wave frequency Ω. These parameters are shown for the anisotropy barrier of the same parameters as in Fig. 2, and for two different strengths of the exchange coupling $\tilde{A}_{mb}$ between the barrier and matrix. The first column (**a**,**c**,**e**) presents the results for an intermediate strength of the coupling (which can be reduced to the case where the natural boundary conditions are applicable – see Supplementary Information), while the second column (**b**,**d**,**f**) shows the results in the regime of week coupling (for which the Hoffmann boundary conditions can be used – see Supplementary Information). Different colours correspond to: tunnelling through the barrier (red), propagation over the barrier (green), propagation in the homogeneous material: matrix (blue) or barrier (black). The calculations have been done for the same values of $\tilde{M}_S = 1$ and $\lambda_{ex} = 1$ in the barrier and in the matrix.

For SWs propagating at frequencies $\Omega > \Omega_b$ (over barrier transmission), the transmissivity T oscillates with increasing Ω, see the maxima (resonances) indicated by the dashed lines in Fig. 2(a,b), for which $|T(\Omega)| = 1$. For $\Omega > \Omega_b$, the modulus of transmissivity, $|T|$, reveals sharp peaks in the regime of weak exchange coupling between the matrix and barrier (region of small interface exchange parameter in Fig. 2a). The weakest oscillations of $|T|$ are observed for moderate values of the interface coupling ($\tilde{A}_{mb} = 1$ in Fig. 2a), corresponding to the natural boundary conditions (NBC) – see Supplementary Information. The oscillation amplitude of $|T|$ increases again with increasing interface exchange parameter, which leads to deeper minima between the resonances. This behaviour can be even more clearly seen in Fig. 3(a,b), where $|T|$ is shown as a function of Ω for two selected values of the interface exchange parameter, corresponding to the natural boundary conditions (Fig. 3a) and a weak interface coupling (Fig. 3b).

The above -described properties of the transmissivity are similar to those observed for tunnelling of other waves existing in nature, including tunnelling of particles in quantum mechanics[24]. The exact correspondence to quantum mechanical tunnelling can be strictly shown for the NBC, when we neglect the contrast of M_S between the matrix and barrier (see Fig. 3a).

The phase acquired in the transmission through (over) the barrier, $\phi = Arg(T) + k_m L$, is an important parameter describing the dynamical properties of wave propagation. Due to the fast changes of ϕ in the frequency domain, we observe large values of the group delay τ_{gr} (see Eqs 13 and 11). From Fig. 2(c,d) one can also notice that the phase ϕ grows (circulates) monotonously with the frequency Ω. Therefore, the group delay is positive as one might expect. The changes of ϕ (and also of τ_{gr}) vary, however, in the frequency domain. In a homogeneous system corresponding, e.g., to the matrix, the phase ϕ_m gained on the distance L is proportional to the wave number k_m, $\phi_m = Lk_m$. Due to a quadratic dispersion relation of the exchange SWs, the phase ϕ_m changes in the frequency domain as $\sqrt{\Omega}$, shifted by a constant value resulting from the static effective field. The magnetic barrier introduces an additional term, $Arg(T)$, to the phase ϕ. This term reflects two features of the barrier, which influence the phase of SWs: (i) the difference in effective anisotropy fields and the contrast of material parameters (saturation magnetization and exchange length), which affect the wave number (see Eqs 9 and 10); (ii) the strength of exchange coupling at the interface between the barrier and matrix included in the boundary conditions (see Supplementary Information), which determines the jump of the phase at these interfaces. For moderate coupling of the barrier and matrix, the correction $Arg(T)$ makes the $\phi(\Omega)$ relation similar to that in the homogeneous system made of the material used to create the barrier, $\phi \approx k_b L$ (see Fig. 3c), with some hardly noticeable deviation close to Ω_b and at the frequencies corresponding to the transmission resonances, where $|T(\Omega)| = 1$ (see the inset in Fig. 3c). These oscillations in the slope of $\phi(\Omega)$ are responsible for the peaks in the group delay τ_{gr}, clearly seen in Fig. 3e. Note that for the homogeneous systems $\tau_{gr}(\Omega)$ decays monotonously with increasing Ω (see the solid blue and dashed black lines in Fig. 3e). The oscillations in $Arg(T)$ are related to the transmissivity resonances, $|T| = 1$. The phase increases approximately by π between two successive resonances (this rule is strict for weak interface exchange coupling). Due to a quadratic dispersion relation ($\Omega \propto k_\alpha^2 = (\phi_\alpha/L)^2$), the distance between successive resonances and peaks of the group delay increases.

The impact of interface exchange coupling and contrast of magnetization (between the barrier and matrix) on the group delay can be deduced from Fig. 2(c,d). The following conclusions can be drawn for the propagation regime ($\Omega > \Omega_b$): For weaker interface exchange coupling $\widetilde{A}_{mb}$ and $\widetilde{M}_S$ in the barrier lower than $\widetilde{M}_S$ in the matrix one finds, (i) the phase ϕ changes more rapidly in the frequency domain and therefore the peaks in τ_{gr} are expected to be higher, and (ii) there are more phase oscillations and more peaks in τ_{gr} per frequency unit. These changes can be attributed to the reduction of spin wave pinning for the weaker interface exchange coupling $\widetilde{A}_{mb}$ and extension of the wavelength in the barrier for lower $\widetilde{M}_S$ inside the barrier.

From Fig. 2(c,d) one can conclude that in the tunnelling regime, $\Omega_m < \Omega < \Omega_b$, the phase changes more rapidly just above the lowest allowed frequency of propagating SWs in the matrix, $\Omega_m = \widetilde{H}_{a,m} + 1$, and just below the frequency Ω_b (determining the threshold between tunnelling and propagation regime). At these frequencies, the slope of the $\phi(\Omega)$ dependence is infinite for homogeneous materials of both the matrix and the barrier. This results in infinite values of the group delay τ_{gr} for homogeneous materials (at the mentioned frequencies), which is supposed to influence the value of τ_{gr} for the system composed of the barrier embedded in the matrix. It is also worth to notice that the phase shift ϕ (between the transmitted and incoming wave) is surprisingly negative for the very low frequencies (close to the Ω_m) and then, it increases for larger frequencies and reaches positive values close to Ω_b.

Figure 3 shows the modulus of the transmissivity $|T(\Omega)|$ (a,b), the phase $\phi(\Omega)$ gained by SW after transmission (c,d), and the corresponding group delay $\tau_{gr}(\Omega)$ (e,f). The numerical results on $\phi(\Omega)$ and $\tau_{gr}(\Omega)$ for the barrier embedded in the matrix are supplemented by the phase of SWs propagating in the homogeneous material of the barrier and matrix, acquired at the distance equal to the width of the barrier, as well as with the plots of the corresponding group delays. These plots have been obtained for the structure without contrast of bulk magnetic parameters ($\widetilde{M}_S$ and λ_{ex}). Using the BMBC we analyzed two special cases: intermediate exchange coupling at the interface, corresponding to the NBC, and weak interface coupling, where the Hoffman boundary conditions (HBC) are applicable[45] – see Supplementary Information. The plots in Fig. 3(a,c) are strictly counterparts of the corresponding plots for electronic waves, reported e.g in ref.[24]. The plots presented in Fig. 3 give more detailed insight into the transmission properties of SWs tunnelling (propagating) through (over) the magnetic barrier. The interesting effect is observed in Fig. 3(b). For a small value of A_{mb}, we can see the resonate transmission of spin waves. It means that in such conditions the barrier region is almost decoupled from the matrix and the transmission peaks are supposed to be sharp even for the spin waves of high frequency propagating over the barrier. For lower frequencies, we observed that the group delay of tunnelling spin waves $\widetilde{\tau}_{gr}$ (red line in Fig. 3(e,f)) is shorter than in uniform space $\widetilde{\tau}_{gr,m}$ (blue line in Fig. 3(e,f)) by the cost of reduction of transitivity $|T|$ (compare the red lines in Fig. 3(a,b)). This difference increases for weaker coupling A_{mb} (compare the red lines in Fig. 3(e,f)).

To discuss the HE one needs to analyze in detail the properties of the considered system in the tunnelling regime. In Fig. 4 we show the absolute value of the transmissivity modulus $|T|$ (a,d), the group delay $\widetilde{\tau}_{gr}$ (b,e), and the corresponding FOM (c,f) – all as a function of frequency Ω and material parameters: interface exchange coupling (a-c) and contrast of saturation magnetization between the barrier and matrix (d–f). All the quantities, that is $|T|$, $\widetilde{\tau}_{gr}$ and FOM, are shown in the logarithmic scale. The yellow regions in this figure correspond to large values of the corresponding parameter.

The observation of HE requires optimally large amplitude of the tunnelling SWs. This means that one should consider spin wave packets in the frequency range not very distant from the threshold frequency Ω_b corresponding to the top of the magnetic barrier. The other requirement is a relatively small value of the group delay, which can allow the detection of SWs after passing the magnetic barrier of a certain width in the presence of damping. The last column in Fig. 4 (see (c,f)) shows the FOM defined as the ratio of tunnelling amplitude and group delay. The yellow regions indicate the range of parameters which are the most suitable for experimental observation of the HE.

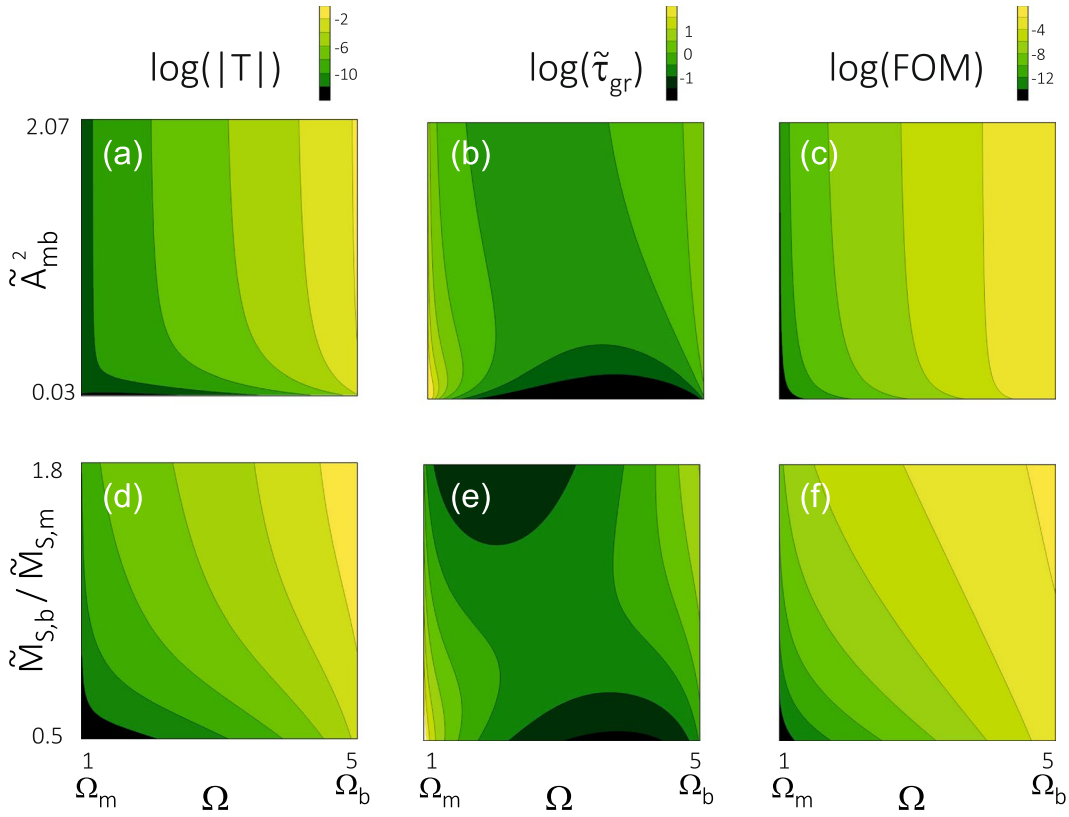

Figure 4. The logarithm of the transmissivity modulus (**a**,**d**), group delay (**b**,**e**), and FOM (**c**,**f**) in the tunnelling regime, $\Omega_m < \Omega < \Omega_b$. All parameters are presented as a function of spin wave frequency Ω and material parameters: the strength of the interface exchange coupling $\widetilde{A}_{mb}$ (**a**–**c**) and the magnetization contrast between the barrier and matrix, $\widetilde{M}_{S,b}/\widetilde{M}_{S,m}$ (**d**–**f**). The calculations have been done for the same values of the exchange length $\lambda_{ex} = 1$ in the barrier and in the matrix. The parameters of the barrier are the same as the ones used in Fig. 2.

The modulus of the transmissivity $|T|$ decays exponentially with decreasing frequency. Therefore, for practical application, only the higher range of frequencies, close to Ω_b, is of some interest. The increase of the interface exchange coupling or saturation magnetization in the barrier can slightly extend this range towards lower frequencies. The group delay, $\tilde{\tau}_{gr}$, reaches the lowest values for intermediate frequencies, between the lowest frequencies for propagating modes in the matrix (here $\Omega_m = 1$) and in the barrier (here $\Omega_b = 5$). The further lowering of $\tilde{\tau}_{gr}$ could be achieved by reducing the interface exchange coupling or saturation magnetization in the barrier (with respect to that in the matrix) – see Fig. 4(b,e). Unfortunately, this change simultaneously leads to a decrease of $|T|$. The better strategy is thus to increase the saturation magnetization contrast by taking larger values of $\widetilde{M}_S$ in the barrier (see Fig. 4e). However, the changes of $\tilde{\tau}_{gr}$ with frequency Ω are not so large as the changes in the transmissivity modulus $|T|$. Therefore, the decisive factor for increasing the FOM, which makes the observation of the HE possible, is the optimization of the modulus of the transmissivity by selection of the frequency range slightly below the threshold value Ω_b, and selection of appropriate values of material parameters (e.g. by the increase of $\widetilde{M}_S$ in the barrier region with respect to that in the matrix).

Now we present the results which demonstrate the HE for the exchange-dominated SWs. Figure 5 shows the saturation of the group delay with increasing barrier width in the tunnelling regime (red curves), which can be considered as a manifestation of the HE. The presented results (Fig. 5) have been obtained for the BMBC, which in the regime of intermediate interface exchange coupling (a,c) and weak exchange coupling (b,d) reduce to the NBC and the HBC, respectively. Let us analyze these results in more details. First, we note that the group delay for the *under-barrier* tunnelling behaves in a different way than that for the *over-barrier* propagation. In the former case, the group delay at small thicknesses L is larger than the time which SW needs to traverse the distance L in the free space (no barrier). In the free space, i.e. in the homogeneous medium made of the matrix material, the group delay increases linearly with the distance, $\tilde{\tau}_{gr,\alpha} = L\frac{dk_\alpha}{d\Omega} = L\nu_{gr,\alpha}$, where $\nu_{gr,\alpha}$ is the group velocity in the homogeneous material. For larger values of L, the group delay increases more slowly than in the case of free motion. Moreover, the group delay saturates with increasing L (see the red lines in Fig. 5(a,b)). In turn, the group delay for the *over-barrier* propagation reveals oscillations with increasing L, but overall it increases linearly with increasing L (see the green curves in Fig. 5a plotted for the NBC, which correspond to an intermediate strength of the interface exchange coupling). The oscillations in the group delay can be significantly stronger in the regime of weak interface exchange coupling, see the green curves in Fig. 5b, where the HBC can be applied. The observed

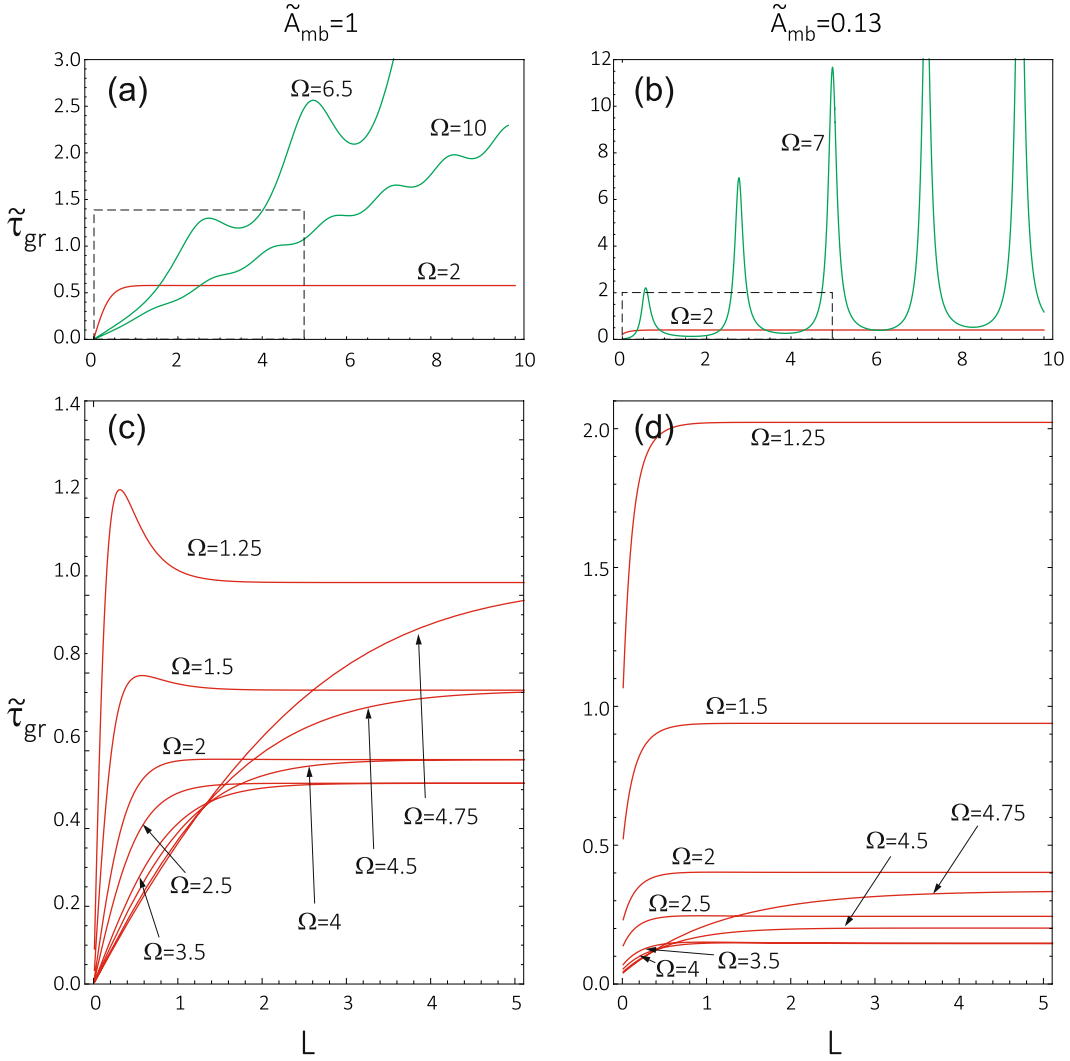

Figure 5. Dependence of the group delay τ_{gr} on the barrier width L for the selected frequencies Ω and for two different strengths of interface exchange coupling $\widetilde{A}_{mb}$ between the barrier and matrix. The first column (**a**,**c**) presents the results for intermediate strength of the coupling (which can be reduced to the case where the natural boundary conditions are applicable). The second column (**b**,**d**) shows the results in the regime of week coupling (for which the Hoffmann boundary conditions can be used). The saturation of the group delay, being the signature of HE, appears in the tunnelling regime ($\Omega_m < \Omega < \Omega_b$) and is shown in more details in (**c**,**d**). The calculations were performed for the same values of $\widetilde{M}_S = 1$ and $A_{ex} = 1$ in the barrier and matrix. The parameters of the barrier are the same as the ones used in Fig. 2.

peaks in $\tilde{\tau}_{gr}$ (and also those in $|T|$) are related to the resonant tunnelling, which can be achieved by the selection of frequency/wavelength or by adjusting the width of the barrier. It is worth to note that even in the regime of weak interface coupling (see the green curves in Fig. 3(b,f)) the linear growth with L is observed both for the maxima of $\tilde{\tau}_{gr}$ peaks and for the minima between them.

In the tunnelling regime (*under-barrier* transmission), the group delay $\tilde{\tau}_{gr}(L)$ saturates with increasing L (see Fig. 5(c,d)). The saturation with increasing L is slower for the higher frequencies which are closer to the threshold value Ω_b. This property makes the observation of the HE difficult because it requires to use wide barriers. Note, that this frequency range is characterized by high values of the FOM, which is beneficial for spin wave transmission. It is also worth to note that for higher, or even intermediate strengths of the interface exchange coupling, the dependence of the group delay on the barrier width is non-monotonous for the lowest frequencies (see the curves for $\Omega = 1.25$, 1.5 in Fig. 5c.

There is one interesting feature of the group delay curves shown in Fig. 5(c,d). Namely, in Fig. 5(c) the group delay vanishes in the limit $L \to 0$, while in Fig. 5(d) a small nonzero value of the group delay remains when $L = 0$. This follows from the fact that although L is reduced to zero, the modified exchange coupling at the barrier/matrix boundaries ($\widetilde{A}_{mb} = 0.13$) remain in Fig. 5(d) when L is reduced to zero. To achieve a uniform system in the limit of $L = 0$ one should also restore the full coupling limit.

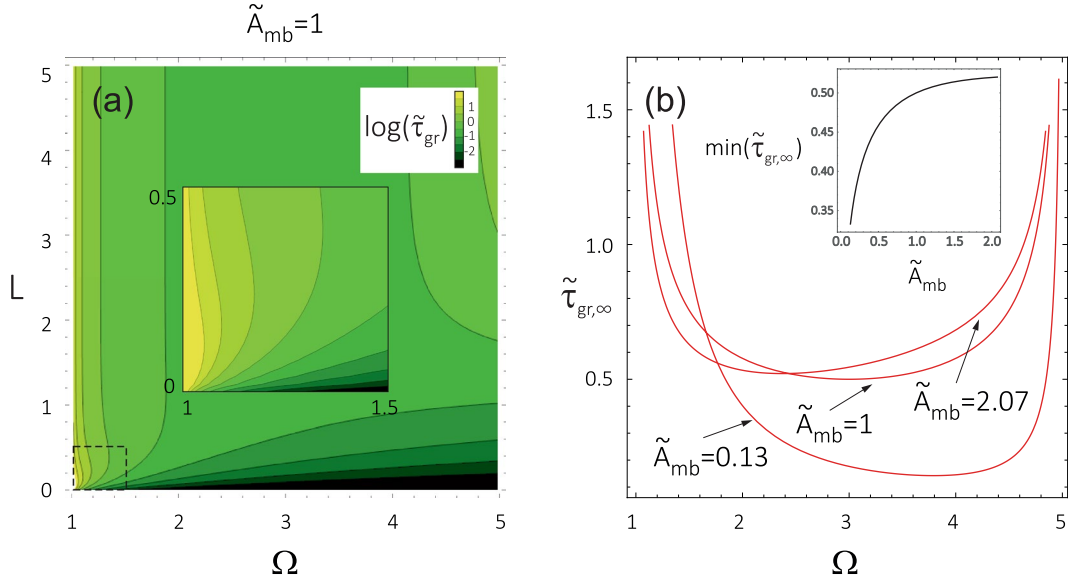

Figure 6. (**a**) Group delay as a function of the barrier thickness and frequency for the natural boundary conditions (see Supplementary Information) applied at the interface between the barrier and matrix. The peculiarities related to the non-monotonous dependence of $\tau_{gr}(L)$ are zoomed in the inset. (**b**) Frequency dependence of the saturation value of the group delay, $\tau_{gr}(L\rightarrow\infty)$, for the indicated values of the exchange coupling between the barrier and matrix $\tilde{A}_{mb}$. The calculations have been done for the same values of $\tilde{M}_S=1$ and $\lambda_{ex}=1$ in the barrier and matrix. The inset in (**b**) presents the dependence of minimal $\tau_{gr}(L\rightarrow\infty)$ on $\tilde{A}_{mb}$. The parameters of the barrier are the same as those used in Fig. 2.

It is clear from Fig. 5(c,d) that the saturation level of the group delay changes with the frequency, displaying a minimum in the tunnelling range $\Omega_m<\Omega<\Omega_b$. This is shown explicitly in Fig. 6. From Fig. 6(a) follows that for the barrier thickness $L=5$ (assumed earlier for calculations presented in Figs 2, 3 and 4), the group delay is almost saturated. Figure 6(a) was obtained for the NBC in the absence of saturation magnetization contrast (like Fig. 3(a,c,e) and Fig. 5(b,c)). We can trace here in detail the effect of reducing the slope of $\tilde{\tau}_{gr}(L)$ with increasing Ω and the non-monotonic character of the $\tilde{\tau}_{gr}(L)$ relation for the lowest frequencies (shown in the inset).

The changes of the saturation level $\tilde{\tau}_{gr,\infty}$ with the frequency Ω are shown even more clearly in Fig. 6(b) for few selected values of the exchange coupling between matrix and barrier: A_{mb}. The minimum of this dependence becomes deeper with decreasing A_{mb} (see inset in Fig. 6(b)), and is shifted towards higher frequencies. The shorter group delay is beneficial for observation of the HE. The better strategy to increase the FOM for the HE is to select the central frequency of tunnelling wave package close to the minimum of the dependence: $\tilde{\tau}_{gr,\infty}(\Omega)$ than to reduce the coupling: A_{mb}. Because the latter approach will result in significant the decrease of the $|T|$.

By reducing $\tilde{\tau}_{gr,\infty}$ we can potentially gain, for narrower barriers, the condition: $\tilde{\tau}_{gr}<\tilde{\tau}_{gr,m}$ (delay time for tunnelling is shorter than the delay in uniform space). This condition is more useful for the experimental search for the signatures of the HE than looking for the saturation of group delay with the increase of the barrier width.

To check how the model described above refers to real systems (see Fig. 1), we performed numerical calculations for a thin layer of CoFeB, which is slightly thinner in the barrier region ($t_{CoFeB,b}=1.0$ nm) than in the matrix area ($t_{CoFeB,m}=1.3$ nm). The saturation magnetization in thin ferromagnetic layers is usually reduced. For the CoFeB layer of the considered thickness, we assumed the following values of M_S: $M_{S,m}=1.2\times10^6$ A/m and $M_{S,b}=0.8\times10^6$ A/m[46]. We also took into account a slight reduction of the exchange stiffness constant in the barrier in reference to its value in the matrix: $A_m=27\times10^{12}$ J/m in the matrix region and $A_b=20\times10^{12}$ J/m in the barrier[46]. To induce the out-of-plane anisotropy, the CoFeB layer is covered by MgO overlayer. For the strong anisotropy of the CoFeB/MgO interface: $K_i=1.3\times10^{-3}$ J/m^2[38], both the matrix and barrier are perpendicularly magnetized, with strong effective anisotropy fields: $\mu_0H_{a,m}=0.16$ T and $\mu_0H_{a,m}=2.24$ T, respectively. We also assumed an external magnetic field $\mu_0H_0=0.5$ T applied perpendicularly to the magnetic layer. The corresponding transmissivity and group delay are shown in Fig. 7 for the barrier width $L=30$ nm. Apart from this, we assumed $t_{mb}=2$ nm for the width of the interface between the matrix and the barrier. At this interface we assumed $M_{S,mb}$ and $\lambda_{ex,mb}$ corresponding to NBC (see Supplementary Information). In the numerical calculation we used the BMBC with the additional term related to surface anisotropy, which was omitted in analytical considerations and which was irrelevant for the results presented in Figs 2–6.

In Fig. 7 we present the transmission characteristics for the high frequency of SWs passing through the anisotropy barrier formed in the CoFeB layer, as described above. Both the transmissivity (Fig. 7(a)) and group delay (7(c)) have typical forms and are similar to those presented in Fig. 3. We were able to adjust the parameters of the model to observe the saturation of the group delay for a relatively narrow barrier, $L=30$ nm. For this width of the barrier we observe noticeable values of $|T|$ in the tunnelling regime for $\gamma\mu_0\omega<H_{a,b}+H_0$ (red part of the plot in Fig. 7(a)). As a result, the FOM which determines the observation possibility of the HE is slightly enhanced. For

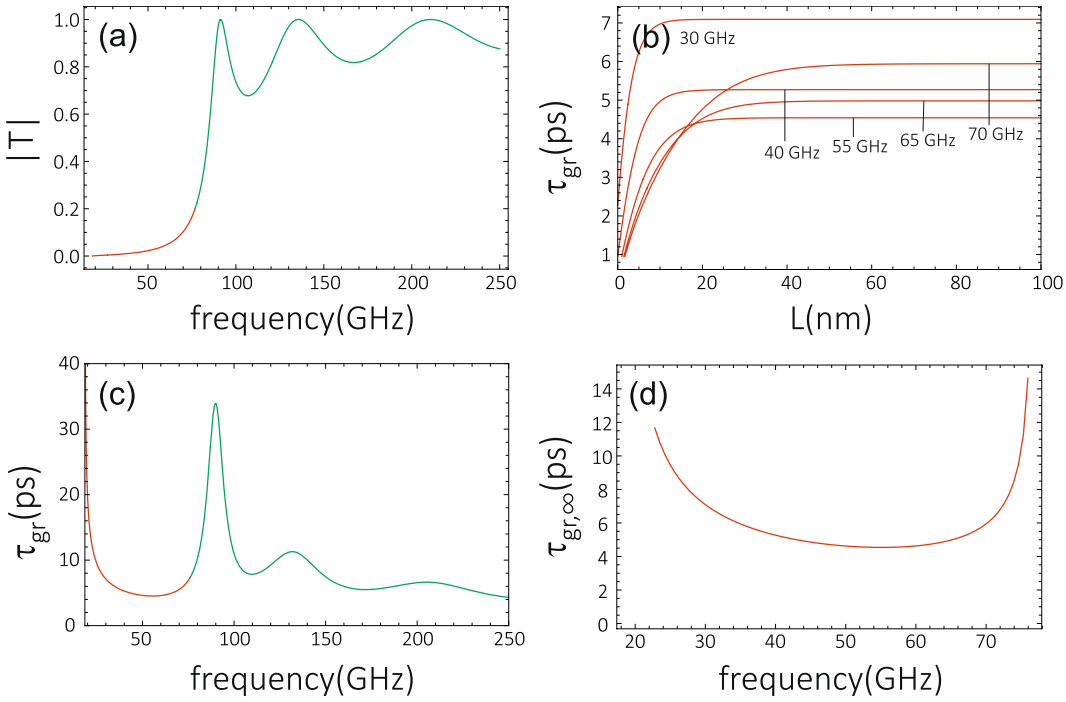

Figure 7. Modulus of the transmissivity $|T|$ (**a**) and the corresponding group delay τ_{gr} (**c**) for the CoFeB layer of thickness $t_{CoFeB,m} = 1.3$ nm and $t_{CoFeB,b} = 1.0$ nm in the matrix and the barrier region, respectively. For $|T|$ and τ_{gr} we assumed the width of the barrier $L = 30$ nm. The thickness of the interface between the matrix and the barrier was assumed as $t_{tm} = 4$ nm. The following material parameters were assumed: $M_{S,m} = 1.2 \times 10^6$ A/m, $M_{S,b} = 0.8 \times 10^6$ A/m, $A_m = 27 \times 10^{12}$ J/m, $A_b = 20 \times 10^{12}$ J/m, $K_i = 1.3 \times 10^{-3}$ J/m^3. The calculations were performed for external field $\mu_0 H_0 = 0.5$ T. Saturation of the group delay τ_{gr}, observed in the tunnelling regime is shown in (**b**). The change of the saturation value of $\tau_{gr,\infty}$ as a function of frequency (**d**) shows the minimum around 55 GHz.

instance, for the frequency $f = 65$ GHz we obtain FOM = 0.16 (cf. Figure 4(c,f)). The relatively small number of the oscillations (resonances) of $|T|$ for $\gamma\mu_0\omega > H_{a,b} + H_0$ (green part of the plot in Fig. 7(a)) results from a relatively narrow width of the barrier assumed here. The larger amplitude of these oscillations originates from the significant contrast of M_S in the matrix and barrier.

Figure 7(b,d) illustrate the occurrence of the HE in the considered system. One can note the saturation of the group delay τ_{gr} for larger widths L of the barrier. The saturation is slower (faster) for higher (lower) frequencies, similarly as in Fig. 5(c,d). By a careful inspection of Fig. 7, one finds that the group delay does not approach zero for $L \to 0$ (see the red dashed lines). This behaviour can be understood when we take into account the fact that the influence of the interface anisotropy field, present in the BMBC, survives in the limit of $L \to 0$, and gives rise to the nonzero values of τ_{gr} in this limit. To get a uniform system in the limit of $L \to 0$, and thus also a vanishing group delay, one should simultaneously adjust the interface anisotropy to that in the matrix.

In the numerical studies the saturation value of $\tau_{gr,\infty}$ was approximated by the group delay τ_{gr} calculated for an extremely wide barrier: L = 200 nm (plotted in Fig. 7(d)). The further extension of the barrier practically does not change τ_{gr}. The dependence of $\tau_{gr,\infty}$ on the frequency, presented in Fig. 7(d), is qualitatively similar to that in Fig. 6(b).

Summary

In this paper, we have analyzed the Hartman effect for high-frequency (few tens of GHz) spin waves tunnelling through a narrow (few tens of nm) magnetic barrier. We investigated a planar system where the barrier was formed by the local increase of a perpendicular magnetic anisotropy. Such an increase may appear due to the specific fabrication of the system – we propose to change the thickness of CoFeB layer covered by MgO to modify spatially the effective out-of-plane anisotropy field. The interesting extension of our studies would be the investigations of the system where the anisotropy in the barrier can be tuned on demand. This can be achieved owing to the magnetostriction effect where, with the aid of piezoelectric transducers, the height of the anisotropy barrier can be adjusted in a certain range by the application an external electric field[47].

By calculating the spin wave transmissivity, we have determined the group delay and found its saturation with increasing barrier width. This proves the existence of the Hartman effect for spin waves. We discussed the impact of exchange boundary conditions (determined by the exchange coupling between the barrier and surrounding material A_{mb}) on the group delay and Hartman effect. We found that decrease of A_{mb} results in the shortening of group delay for tunnelling spin waves by the cost of the reduction of the transitivity.

One should mention that for an exchange dominated system the shape of the transmitted and reflected wave packets is remarkably modified, which follows from the frequency dependence of the transmissivity. This problem can be solved when we consider the tunnelling of dipolar spin waves which can be characterized by linear dispersion relation in range of small wave vectors. However, in the dipolar regime we are limited to lower operating frequencies and restricted to larger sizes of the devices (due to the increase in their wavelengths).

References

1. Landau, L. D. & Lifshitz, E. M. *Quantum Mechanics* (Butterworth-Heinemann, Oxford, 2004).
2. Messiah, A. Quantum Mechanics (Elsevier, Amsterdam, 2006).
3. Roy, D. K. *Quantum Mechanical Tunneling and its Applications* (World Scientific Publishing, Philadelphia, 1986).
4. Olkhovsky, V., Recami, E. & Jakiel, J. Unified time analysis of photon and particle tunneling. *Phys. Rep.* **398**, 133 (2004).
5. Hartman, T. E. Tunneling of a wave packet. *J. Appl. Phys.* **33**, 3427 (1962).
6. Olkhovsky, V. S. & Recami, E. Recent developments in the time analysis of tunneling processes. *Phys. Rep.* **214**, 339 (1992).
7. Winful, H. Physical mechanism for apparent superluminality in barrier tunneling. *IEEE J. Sel. Top. Quant. Electron.* **9**, 17 (2003).
8. Winful, H. G. Nature of "superluminal" barrier tunneling. *Phys. Rev. Lett.* **90**, 023901 (2003).
9. Schwartsburg, A. B. Tunneling of electromagnetic waves: paradoxes and prospects. *Phys.-Usp.* **50**, 37 (2007).
10. Niemtz, G. & Heitman, W. Superluminal photonic tunneling and quantum electronics. *Phys.-Usp.* **21**, 81 (1997).
11. Niemtz, G. On superluminal tunneling. *Prog. Quant. Electron.* **27**, 417 (2003).
12. Olkhovsky, V. On the multiple internal reflections of particles and photons tunneling in one, two, or three dimensions. *Phys.-Usp.* **57**, 1136 (2014).
13. Wang, L.-G., Xu, J.-P. & Zhu., S.-Y. Negative hartman effect in one-dimensional photonic crystal with negative refractive materials. *Phys.Rev.E* **70**, 066624 (2004).
14. Sahrai, M., Aghaei, R., Sattari, H. & Poursamad, J. Hartman effect in a doped one-dimensional photonic crystal at normal ad oblique incidence. *J. Opt. Soc. Am. B* **32**, 751 (2015).
15. Dadoenkova, Y. S. *et al*. Tunnelling of frequency-modulated wavepackets in photonic crystals with amplification. *J. Opt.* **18**, 015102 (2016).
16. Jamil, R., Ali, A. B., Abbas, M., Badshah, F. & Qamar, S. Phase time delay and Hartman effect in a one-dimensional photonic crystal with four-level atomic defect layer. *J.Mod.Opt.* **64**, 1457 (2017).
17. Huynh, A. *et al*. Sub terahertz phonon dynamics in acoustic nanocavities. *Phys.Rev.Letts.* **97**, 115502 (2006).
18. Villegas, D., Arriaga, J., León-Pérez, F. & Pérez-Álvarez, R. Goos-Hänchen effect for optical vibrational modes in a semiconductor structure. *J. Phys.: Condens. Matter.* **29**, 125301 (2017).
19. Wu, Z., Chang, K., Liu, J. T., Li, X. J. & Chan, K. S. The Hartman effect in graphene. *J. Appl. Phys.* **105**, 043702 (2009).
20. Sepkhnov, R. A., Medvedyeva, M. V. & Beenakker, C. V. J. Hartman effect and spin precession in graphene. *Phys. Rev. B* **80**, 245433 (2009).
21. Park, C.-S. Chiral tunneling, tunneling times, and Hartman effect in bilayer graphene. *Phys. Rev. B* **89**, 115423 (2014).
22. Chen, X., Deng, Z.-Y. & Ban, Y. Delay time and Hartman effect in strain engineered graphene. *J. Appl. Phys.* **115**, 173703 (2014).
23. Ban, Y., Wang, L.-J. & Chen, X. Tunable delay time and Hartman effect in graphene magnetic barriers. *J. Appl. Phys.* **117**, 164307 (2015).
24. Winful, H. G. Tunneling time, the Hartman effect, and superluminality: A proposed resolution of an old paradox. *Phys. Rep.* **436**, 1 (2006).
25. Büttiker, M. & Washburn, S. Ado about nothing much? *Nat.* **422**, 271 (2003).
26. Winful, H. G. Energy storage in superluminal barrier tunneling: Origin of the "Hartman effect". *Opt. Express* **10**, 1491 (2002).
27. Demokritov, S. *et al*. Tunneling of dipolar spin waves through a region of inhomogeneous magnetic field. *Phys. Rev. Lett.* **93**, 047201 (2004).
28. Hansen, U.-H., Gatzen, M., Demidov, V. E. & Demokritov, S. O. Resonant tunneling of spin-wave packets via quantized states in potential wells. *Phys. Rev. Lett.* **99**, 127204 (2007).
29. Schneider, T. *et al*. Spin-wave tunnelling through a mechanical gap. *Eur. Lett.* **90**, 27003 (2010).
30. Bankowski, E. *et al*. Magnonic crystal as a delay line for low-noise auto-oscillators. *Appl. Phys. Lett.* **107**, 122409 (2015).
31. Chumak, A. V. *et al*. Storage-recovery phenomenon in magnonic crystal. *Phys. Rev. Lett.* **108**, 257207 (2012).
32. Neusser, S. *et al*. Magnonic minibands in antidot lattices with large spin-wave propagation velocities. *Phys. Rev. B* **84**, 094454 (2011).
33. Tacchi, S. *et al*. Universal dependence of the spin wave band structure on the geometrical characteristics of two-dimensional magnonic crystals. *Sci. Rep.* **5**, 10367 (2015).
34. Dadoenkova, Y. S. *et al*. Huge Goos-Hänchen effect for spin waves: A promising tool for study magnetic properties at interfaces. *Appl. Phys. Lett.* **101**, 042404 (2012).
35. Götte, J. B. & Dennis, M. R. Generalized shifts and weak values for polarization components of reflected light beams. *New J. Phys.* **14**, 073016 (2012).
36. Gruszecki, P. *et al*. Goos-Hänchen effect and bending of spin wave beams in thin magnetic films. *Appl. Phys. Lett.* **105**, 242406 (2014).
37. Gruszecki, P. *et al*. Influence of magnetic surface anisotropy on spin wave reflection from the edge of ferromagnetic film. *Phys. Rev. B* **92**, 054427 (2015).
38. Ikeda, S. *et al*. A perpendicular-anisotropy CoFeB–MgO magnetic tunnel junction. *Nat. Mater.* **9**, 721 (2010).
39. Zhu, T., Zhang, Q. & Yu, R. Tuning perpendicular magnetic anisotropy in the MgO/CoFeB/Ta thin films. *arXiv:1405.2551* (2014).
40. Krawczyk, M., Sokolovskyy, M., Kłos, J. & Mamica, S. On the formulation of the exchange field in the Landau-Lifshitz equation for spin-wave calculation in magnonic crystals. *Adv. Condens. Matter Phys.* **2012**, 764783 (2012).
41. Barnaś, J. On the Hoffmann boundary conditions at the interface between two ferromagnets. *J. Magn. Magn. Mater.* **102**, 319–322 (1991).
42. Mills, D. L. Spin waves in ultrathin exchange-coupled ferromagnetic multilayers: The boundary condition at the interface. *Phys. Rev. B* **45**, 13100–13104 (1992).
43. Falck, J. P. & Hauge, E. H. Larmor clock reexamined. *Phys. Rev. B* **38**, 3287–3297 (1988).
44. Winful, H. G. Delay time and the hartman effect in quantum tunneling. *Phys. Rev. Lett.* **91**, 260401 (2003).
45. Hoffmann, F., Stankoff, A. & Pascard, H. Evidence for an exchange coupling at the interface between two ferromagnetic films. *J. Appl. Phys.* **41**, 1022–1023 (1970).
46. Devolder, T. *et al*. Exchange stiffness in ultrathin perpendicularly magnetized CoFeB layers determined using the spectroscopy of electrically excited spin waves. *J. Appl. Phys.* **120**, 183902 (2016).
47. Ota, S. *et al*. Strain-induced reversible modulation of the magnetic anisotropy in perpendicularly magnetized metals deposited on a flexible substrate. *Appl. Phys. Express* **9**, 043004 (2016).

Acknowledgements

The study has received financial support from the National Science Centre of Poland Grants No.: UMO-2016/21/B/ST3/00452, UMO-2017/24/T/ST3/00173 and the EU's Horizon 2020 Research and Innovation Program under Marie Skłodowska – Curie Grant Agreement No. 644348 (MagIC). J.W.K., J.R., Y.S.D. and N.N.D. would like to acknowledge the support of the Foundation of Alfried Krupp Kolleg Greifswald, the Adam Mickiewicz University Foundation and the Ministry of Education and Science of the Russian Federation: State Contract No. 3.7614.2017/9.10 and project No. 14.Z50.31.0015, respectively. Y.S.D., N.N.D. and I.L.L. acknowledge also the support from the grant: COST Action MP1403 (Nanoscale Quantum Optics). The authors would like to thank Prof. M. Krawczyk for remarks and discussion.

Author Contributions

J.B. and I.L.L. brought the idea to consider the Hartman effect for spin waves and proposed the theoretical model for study of this phenomenon, J.W.K. did most of theoretical work, Y.S.D., J.R., N.N.D. analyzed the results and preformed the numerical calculations. All authors participated in discussion and reviewed the manuscript.

Additional Information

Supplementary information accompanies this paper at https://doi.org/10.1038/s41598-018-35761-1.

Competing Interests: The authors declare no competing interests.

Publisher's note: Springer Nature remains neutral with regard to jurisdictional claims in published maps and institutional affiliations.